Photoluminescence Hot Paper

International Edition: DOI: 10.1002/anie.201508276
German Edition: DOI: 10.1002/ange.201508276

Colloidal $CsPbBr_3$ Perovskite Nanocrystals: Luminescence beyond Traditional Quantum Dots

*Abhishek Swarnkar, Ramya Chulliyil, Vikash Kumar Ravi, Mir Irfanullah, Arindam Chowdhury, and Angshuman Nag**

Abstract: *Traditional CdSe-based colloidal quantum dots (cQDs) have interesting photoluminescence (PL) properties. Herein we highlight the advantages in both ensemble and single-nanocrystal PL of colloidal $CsPbBr_3$ nanocrystals (NCs) over the traditional cQDs. An ensemble of colloidal $CsPbBr_3$ NCs (11 nm) exhibits ca. 90% PL quantum yield with narrow (FWHM = 86 meV) spectral width. Interestingly, the spectral width of a single-NC and an ensemble are almost identical, ruling out the problem of size-distribution in PL broadening. Eliminating this problem leads to a negligible influence of self-absorption and Förster resonance energy transfer, along with batch-to-batch reproducibility of NCs exhibiting PL peaks within ± 1 nm. Also, PL peak positions do not alter with measurement temperature in the range of 25 to 100°C. Importantly, $CsPbBr_3$ NCs exhibit suppressed PL blinking with ca. 90% of the individual NCs remain mostly emissive (on-time > 85%), without much influence of excitation power.*

The $CsPbX_3$ (X = Cl, Br, or I) perovskite was reported by Møller in 1958.[1] Mitzi and co-workers showed the interesting optoelectronic properties of organic–inorganic perovskite materials about twenty years ago.[2] In about the last six years, solution-processed organic–inorganic hybrid perovskites, such as $CH_3NH_3PbI_3$, became one of the most celebrated materials because they exhibit nearly 20% solar-cell efficiency.[3] This success of bulk perovskite, also prompted a few reports on colloidal nanocrystals (NCs) of $MPbX_3$ (M = CH_3NH_3 and Cs; X = Cl, Br, and I), where intense photoluminescence (PL) has been the main property.[4] Herein, we establish that PL from $CsPbBr_3$ perovskite NCs is intrinsically different and advantageous, compared to that from traditional colloidal quantum dots (cQDs).

State of the art, highly luminescent CdSe-based cQDs, particularly, core–shell NCs found applications in high-definition displays because of the narrower full width at half maxima (FWHM) of their PL compared to that of organic dyes.[5] Kovalenko et al.[4b] reported early this year that $CsPbX_3$ (X = Cl, Br, and I) NCs exhibit around 90% PL efficiency with narrow FWHM, which is superior to most CdSe-based NCs obtained even after surface modifications.

Traditional CdSe based cQDs exhibit intense PL only when the size of NC (ca. 5 nm) is comparable to the Bohr excitonic diameter, where strong quantum confinement of charge carriers enhances the transition probability. This requirement of quantum confinement, however, results into spectral broadening from the size-distribution, and a high density of trap states because of the large surface to volume ratio.[6] Owing to the size-distribution problem where smaller sized NCs exhibit higher optical gap compared to larger sized ones, chromaticity and quantum yield (QY) of PL changes with concentration of NCs because of both self-absorption and Förster resonance energy transfer (FRET).[7] Also, since the optical gap of such luminescent cQD is strongly dependent on the size of the NCs, reproduction of NC synthesis to give a PL peak position within an error of ± 5 nm is often challenging. Another disadvantage of CdSe-based cQDs for light-emitting device (LED) applications is a decrease in optical gap with increasing temperature that can change the chromaticity of an LED with operational temperature.

Our results show that PL from an ensemble of $CsPbBr_3$ NCs does not suffer from any of these above mentioned demerits of traditional cQDs, while maintaining around 90% PL QY. To understand luminescence from $CsPbBr_3$ NCs, we studied the PL behaviors of individual NCs.[8] Surprisingly, the spectral line-width (FWHM) of single NCs is almost identical with that of ensemble. Further, the majority of individual $CsPbBr_3$ NCs exhibit considerable suppression of PL intermittency (blinking) under ambient conditions, compared to traditional cQDs.

Colloidal $CsPbBr_3$ NCs with cubic morphology[4b] and orthorhombic crystal structure were prepared. Details of synthesis and characterization of different sizes of $CsPbBr_3$ NCs using transmission electron microscopy (TEM), UV/Vis absorption and PL spectra are given in Figure 1a and Figure S1–S2 of Supporting Information. TEM image in Figure 1a shows the average edge length of $CsPbBr_3$ cubes is 11 nm. The powder X-ray diffraction (XRD) pattern in Figure 1b shows orthorhombic phase of $CsPbBr_3$ NCs, similar to bulk $CsPbBr_3$,[9] but differs from Ref. [4b] that suggested cubic phase for $CsPbBr_3$ NCs. We note that, for smaller $CsPbBr_3$ NCs with broadened XRD peaks, it is difficult to distinguish between cubic and orthorhombic phases both exhibiting similar Bragg's angles for intense peaks. Furthermore, differential scanning calorimetry (DSC) data of our NCs in the inset of Figure 1b agrees with that reported[9] for bulk $CsPbBr_3$, suggesting an orthorhombic to tetragonal

[*] A. Swarnkar, V. K. Ravi, Dr. A. Nag
Department of Chemistry
Indian Institute of Science Education and Research (IISER)
Pune 411008 (India)
E-mail: angshuman@iiserpune.ac.in
R. Chulliyil, Dr. M. Irfanullah, Dr. A. Chowdhury
Department of Chemistry, Indian Institute of Technology Bombay
Powai, Mumbai 400076 (India)

Supporting information for this article is available on the WWW under http://dx.doi.org/10.1002/anie.201508276.

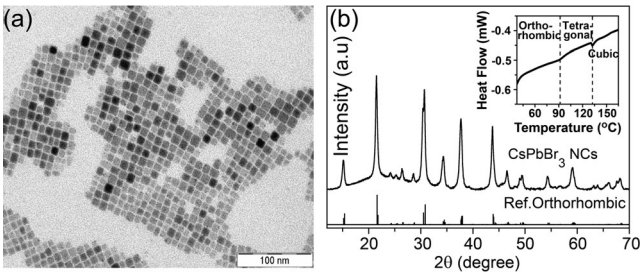

Figure 1. a) TEM image and b) powder XRD pattern of $CsPbBr_3$ NCs exhibiting cubic morphology with an edge length of 11 nm. Inset: DSC data of the same sample.

transition at about 91 °C, and tetragonal to cubic transition at around 132 °C. Figure S2 shows a nominal (20 meV) blue shift in the absorption edge and emission maxima on decreasing the edge length of $CsPbBr_3$ cubes from 11 to 8 nm, suggesting weak quantum confinement of charge carriers in this size regime, which agrees with the reported[4b] approximate 7 nm excitonic Bohr diameter.

Our 11 nm $CsPbBr_3$ NC dispersion was found to exhibit the best PL QY of 90%, and is studied more extensively below. Figure 2a shows the spectral shapes of PL originating

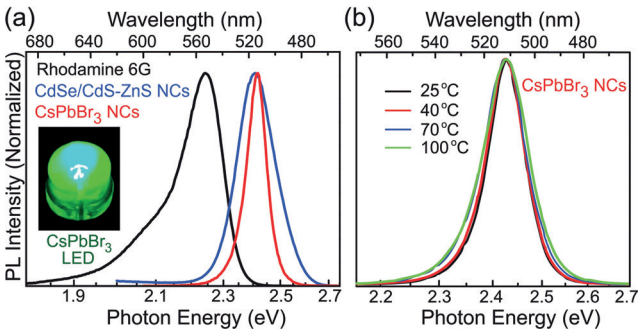

Figure 2. a) PL spectral line widths obtained from a representative organic dye Rhodamine 6G, CdSe/CdS-ZnS core/hybrid-shell NCs, and $CsPbBr_3$ NCs. Inset: photograph of a green LED obtained after coating an UV-LED with $CsPbBr_3$ NCs. b) Variation in PL spectra of colloidal $CsPbBr_3$ NCs with measurement temperature.

from organic dye Rhodamine 6G, CdSe/CdS-ZnS core/hybrid-shell NCs (prepared following Ref. [10]), and $CsPbBr_3$ NCs. Clearly, $CsPbBr_3$ NCs exhibit the best color purity of emitted light with narrowest FWHM (86 meV). Such a narrow FWHM, along with 90% PL QY, makes these $CsPbBr_3$ NCs suitable for application in high-definition displays. Inset to Figure 2a shows a photograph of a green LED prepared by coating $CsPbBr_3$ NCs on top of a UV (365 nm) LED. The green LED continues to emit intense light after 3 months from the date of coating, even when stored under ambient conditions.[11] Also, Figure S3 shows that the PL from colloidal $CsPbBr_3$ NCs is stable under prolonged exposure to UV light. Another advantage is the batch to batch reproducibility in the synthesis of $CsPbBr_3$ NCs with the optical gap lying within ± 1 nm. Not only the PL peak position but the QYs of $CsPbBr_3$ NCs are also reproducible (Figure S4).

The optical gap of a semiconductor usually decreases with increasing temperature.[12] The PL spectra of colloidal CdSe NCs (Figure S5) and CdSe/CdS-ZnS core/hybrid-shell NCs (Figure S6) systematically red-shift by 30 meV (8 nm), and 40 meV (9 nm) respectively, upon increasing the measurement temperature from 25 °C to 100 °C. Such a temperature-dependent increase in emission energy can change the chromaticity of an LED, since the device heats up during prolonged operation. Interestingly, $CsPbBr_3$ NCs (Figure 2b) do not exhibit any change in PL peak position in this temperature range. This unusual behavior can be attributed to the electronic structure of $CsPbBr_3$, where the optical gap predominantly arises from the 6s to 6p transition of Pb^{2+}, with less influence from Br^-.[12] Therefore, thermal expansion of the lattice which would decrease the cation–anion interaction, does not decrease the optical gap.[12] Further theoretical and experimental studies over a wider temperature range are required for a better understanding of this behavior.

Another aspect of traditional cQDs is self-absorption and FRET.[7] For example, Figure 3a shows the red-shift in the PL of CdSe/CdS-ZnS core/hybrid-shell NC film, compared to its dilute dispersion in toluene. Such red-shifts in close-packed films happens either because higher energy light emitted by a smaller NC is re-absorbed (self-absorption) by a larger NC with a smaller optical gap, and/or the excited smaller NC non-radiatively (FRET) transfers its energy to a larger NC. Such processes dominate at high concentrations (closer proximity) of NCs. Figure 3a also shows a decrease in the relative PL intensity for CdSe/CdS-ZnS core/hybrid-shell NC film com-

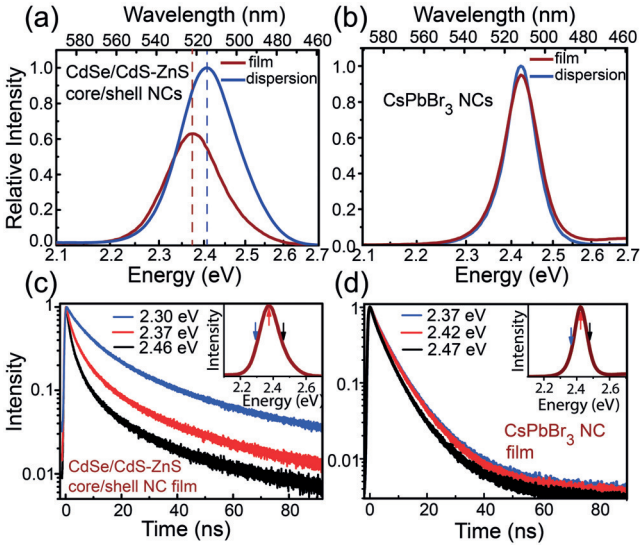

Figure 3. PL spectra for a) CdSe/CdS-ZnS core/hybrid-shell NCs, and b) $CsPbBr_3$ NCs dispersed in toluene and a film of the same NCs on a quartz substrate. PL intensities were compared after normalizing with absorbance at the excitation wavelength 3.1 eV (400 nm). For films, absorption and PL data were collected at 10 different locations of the film, averaged spectra are plotted to minimize the error that can arise because of inhomogeneity in film thickness. PL decay profiles obtained from films of c) CdSe/CdS-ZnS core/hybrid-shell NCs, and d) $CsPbBr_3$ NCs at different emission wavelengths as mentioned in each panel. Insets: corresponding PL spectrum indicating the emission wavelengths by color coded arrows.

pared to the corresponding dilute dispersion. This decrease is because some of the larger NCs that were excited at the cost of emission from the smaller NCs, might be non-emitting (or poorly emitting) NCs. On the other hand, (Figure 3b) both peak position and relative intensity of $CsPbBr_3$ NCs remained almost identical for both close-packed film and dilute dispersion. This observation suggests that both self-absorption and FRET do not influence the PL spectrum of the $CsPbBr_3$ NC film.

PL decay dynamics in Figure 3c show that film of CdSe/CdS-ZnS core/hybrid-shell NCs systematically exhibits faster decay at higher emission energies, unlike the PL decay profile of its dilute dispersion (Figure S7). This faster decay at higher energies is because of smaller NCs that emit at higher energies exhibit an additional FRET-related decay channels. In contrast, closed-packed film of $CsPbBr_3$ NCs in Figure 3d show similar PL decay at all emission energies. Such similarities suggest that contribution from FRET is less in the case of the $CsPbBr_3$ NC film. Figure S8 shows that the absorption tail at energies lower than the lowest energy excitonic absorption peak of $CsPbBr_3$ NCs is significantly less intense compared to that for the CdSe/CdS-ZnS core/hybrid-shell NCs. This sharp rise in the excitonic absorption of $CsPbBr_3$ can explain the suppression of FRET, and agrees with both the absence of size-distribution related broadening of optical gap, and the small Urbach energy reported[3e] for bulk lead-halide perovskites.

PL decays from $CsPbBr_3$ NC film at different emission energies were fitted with a bi-exponential decay (Figure S9 and Table S1) exhibiting 3 ns and 8 ns radiative lifetimes, with nearly equal contributions. We do not observe sub-ns non-radiative decay channels agreeing with the nearly ideal PL QY. These short radiative lifetimes, along with the observed excitonic features in absorption spectrum (Figure S2a) suggest that the PL from $CsPbBr_3$ NCs originates from excitonic recombination, unlike the recent reports[13] of bulk $CH_3NH_3PbI_3$, where recombination of free electron and hole has been proposed to give rise to the PL. This excitonic PL from $CsPbBr_3$ NCs can be explained by both higher exciton binding energy for bulk $CsPbBr_3$ (35–40 meV) and confinement charge carriers in NCs.[4b]

To understand the PL of $CsPbBr_3$ NCs in detail, we investigated the behaviors of individual NCs cast on a silica substrate. Figure 4a shows a typical PL image of spatially segregated single NCs, for which an extremely high signal to background ratio (>20) is frequently observed. So intense is the PL that individual $CsPbBr_3$ NCs could be imaged at both very low ($1\ W\,cm^{-2}$) excitation power and 10 ms exposure time, while in our wide-field setup, detection of single CdSe/CdS-ZnS core/hybrid shell QDs require much higher powers as well as exposure times. Clearly, the intense brightness of $CsPbBr_3$ NCs allows for the acquisition of high quality single-NC emission spectra with reasonable ease (Figure S10 and movie SM1). Figure 4b shows PL spectrum of a representative single-NC (several such spectra are provided in Figure S10) along with the average spectra of 90 single-NCs, and, for comparison, the PL spectrum from an ensemble of $CsPbBr_3$ NCs in solution. Remarkably, FWHM of both the single-NC spectrum (75 meV) as well as for the sub-ensemble

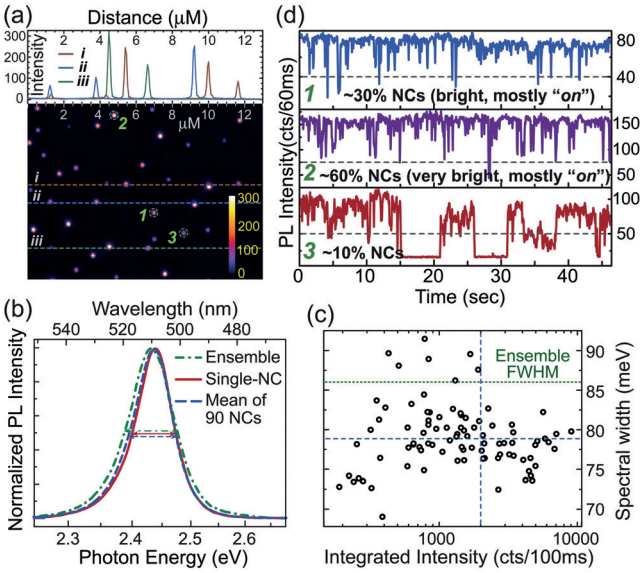

Figure 4. a) PL image of single $CsPbBr_3$ NCs at excitation power of $9\ W\,cm^{-2}$ and 60 ms exposure time; intensity line profiles show extremely high signal to background b) Normalized PL emission spectra of an ensemble of NCs in solution (green dashed dot line) and a representative single-NC (red solid line) along with the sum of 90 single NC spectra (blue dashed line); Arrows depict spectral linewidths. c) Scatter plot of spectral FWHM and spectrally integrated intensity for 90 single NCs; Dashed lines represent average values of integrated intensities (vertical line) and FWHM (horizontal line) for 90 NCs. d) Characteristic temporal fluctuation of PL intensity for three typical single NCs marked (*1-3*) in (a), along with proportion of NCs (for several hundred single NCs studied) which exhibit corresponding intensity/blinking behaviors; Dashed lines mark approximately 50% intensity compared to the "bright" level. Movies SM 2–4 are provided in the Supporting Information, along with a movie (SM5) collected at higher frame rate of 40 Hz.

of 90 individual NCs (78 meV) are only slightly smaller than that of the ensemble (86 meV). For the majority of single-NCs, the FWHM are spread over a rather narrow window of 72–85 meV (mean ca. 79 meV), without any systematic dependence on emission intensity (Figure 4c), which illustrate that the detrimental effect of size-distribution in broadening of ensemble PL spectrum is nominal for $CsPbBr_3$ NCs.

Our 11 nm $CsPbBr_3$ NCs are slightly larger than the corresponding Bohr excitonic diameter of 7 nm, exhibiting weak quantum confinement effect on charge carriers. This weak nature of confinement, along with the narrow size-distribution obtained, ensures that the individual $CsPbBr_3$ NCs within an ensemble exhibit almost identical optical gaps. On the other hand, traditional cQDs require a stronger confinement of charge carriers to exhibit high PL QY,[6] where a larger inhomogeneity in the optical gaps of the NCs within an ensemble arises even after achieving a narrow size distribution. For example, ensemble CdSe NCs with a size larger than the excitonic diameter show homogeneity in optical gap but do not exhibit intense luminescence. In the case of $CsPbBr_3$ NCs, weak confinement of charge carrier is sufficient enough to exhibit high transition probability for luminescence. Nearly identical effective mass of

electron ($m_e = 0.15$ electron mass) and hole ($m_h = 0.14$ electron mass),[4b] will lead to an equal extent of confinement for both charge carriers, which in turn is expected to increase the transition probability for PL by increasing the overlap between electron and hole wavefunctions. Detailed theoretical studies on the quantum confinement effect of such perovskite NCs are required for a better understanding. The fact that PL is not much influenced by the size-distribution of the 11 nm $CsPbBr_3$ NCs, explains our observations such as 1) narrow FWHM of ensemble, 2) batch to batch reproducibility, and 3) negligible influence of self-absorption and FRET on emission energy. This weak confinement on the other hand will inhibit significant size-dependent tuning of emission color, which can be overcome by controlling the composition of $CsPbX_3$, where X can be a combination of Cl, Br, and I.[4b]

Interestingly, we find that individual $CsPbBr_3$ NCs undergo unambiguous temporal fluctuations in their PL emission under continuous illumination (Figure 4d and movies SM2–SM4). Although PL intermittency (blinking) has been recently observed for large (ca. 200 nm) perovskite NCs[14a] as well for perovskite NC films,[14] there are hardly any reports on blinking of such small (ca. 10 nm) quantum-confined perovskite NCs. Figure 4d shows the blinking characteristics along with the fraction of single $CsPbBr_3$ NCs that exhibit similar nature of PL intermittency. Importantly, the vast majority (ca. 90%) of several hundred individual NCs studied display substantial blinking suppression, that is, remain mostly emissive (on-time $> 85\%$), and the nature of blinking is not severely affected over a wide range of excitation powers (Figure S11 and movies SM2–SM4). In addition, rather than abrupt switching to a completely non-emissive state, most of the NCs exhibit frequent flickering (dimming), where the emission intensity vacillates between "bright" and "dim" levels with very short (< 60 ms) dim-time bursts (Figure S11). Such flickering behaviors are in stark contrast to conventional CdSe-based core–shell cQDs, where clear fluctuations in emission intensity occur between a bright (on) and a dark (off) level, and on-/off-time durations as well as the net on/off ratio for individual NCs depend on the density of photo-generated carriers.[8] That the NCs mostly flicker and rarely blink to "off" levels implies that the time durations for complete absence of emission does not exceed a few tens of milliseconds, which was corroborated by collecting single-NC movies at 40 Hz (Movie SM5).

Intriguingly, we find that initially, all the single NCs are almost non-emissive and remain in a dark state. However, upon continuous illumination, radiative recombination is initiated (over seconds) and near saturation brightness is achieved almost instantly, within few hundreds of milliseconds of the advent of PL emission (Movie SM6). Further, after initial illumination (for 1 min), when kept in the dark (for 1 min) the PL emissions from the same NCs are quenched completely (for the vast majority), and emission resumes after a delay upon exposure to light (Movie SM7). This provides evidence on photoinduced activation of NCs and slow-timescale (tens of seconds) deactivation processes in the absence of radiation. While the origins of this phenomenon still remain unclear, it is likely that such temporally delayed initiation of radiative emission for these perovskite NCs is due to saturation of non-radiative traps (quenchers) within individual NCs, similar to that recently observed for localized emission centers within $CH_3NH_3PbI_3$ microcrystals.[14a] We also noticed that upon constant laser illumination under ambient conditions, the PL spectra of a fraction (ca. 25%) of individual $CsPbBr_3$ NCs underwent continuous blue shift to different extents (Figure S12). While such a temporal shift in energy may be due to photo-oxidation of NCs, further study is necessary to pinpoint the reasons behind both initial photo-triggered emission enhancement and subsequent spectral blue-shifts with further illumination.

In conclusion, we have highlighted advantageous PL behavior of $CsPbBr_3$ NCs compared to traditional cQDs. 90% PL QY with narrow (86 meV) FWHM, negligible influence of FRET and self-absorption, temperature-independent chromaticity, and batch to batch reproducibility suggest that our $CsPbBr_3$ NCs can be a better candidate for high-definition displays than traditional cQDs. The key aspect that leads to improved PL behavior of $CsPbBr_3$ NCs is that such NCs exhibit strong excitonic PL when the charge carriers are just weakly confined, and excitonic transition energy is less sensitive to NC size. The FWHM of single-NC PL (78 meV) is almost same as that of ensemble of $CsPbBr_3$ NCs, signifying that size-distribution does not broaden the PL spectrum of the ensemble. Temporal PL behavior shows suppression of blinking-off states, but exhibits flickering in the high intensity level. In fact, approximately 90% of the individual $CsPbBr_3$ NCs remain emissive (on-time $> 85\%$) without much influence of excitation power. Such suppression of blinking will be useful for single-NC-based super-resolution PL imaging.

Experimental Section

Colloidal $CsPbBr_3$ NCs were synthesized following the procedure in Ref. [4b] A magnetically stirred mixture of $PbBr_2$ (0.188 mmol) with 5 mL dried 1-octadecene (ODE) was degassed (under alternate vacuum and nitrogen) at 120 °C for 60 min. Dried oleic acid and oleylamine, each 0.5 mL, was added to the mixture at 120 °C. After ca. 30 min, $PbBr_2$ is dissolved in ODE and then the temperature was increased to 190 °C. Cs-oleate (0.1M, 0.4 mL) solution in 1-octadecene, pre-heated at 100 °C, was swiftly injected to the reaction mixture. The reaction mixture became greenish and the reaction was stopped by dipping the reaction flask into an ice bath. The synthesized $CsPbBr_3$ NCs were precipitated by adding 5 mL *tert*-butanol at room temperature and then centrifuged at 7000 rpm. Finally, the wet pellet of the NCs was redispersed in 5 mL toluene for characterization. The obtained NCs were cubic in shape with length 11 nm. To achieve smaller sized NCs (cube with 8 nm length), the reaction temperature was kept at 165 °C. Other experimental details, including single-NC spectroscopy and microscopy are provided in the Supporting Information along with supporting figures and movies.

Acknowledgements

A.N. acknowledges Science and Engineering Research Board (SERB) Govt. of India, for Ramanujan Fellowship (SR/S2/RJN-61/2012). A.C. thanks IRCC, IIT Bombay, and MNRE (Govt. of India) funded NCPRE for partial financial support.

R.C. and M.I. thank UGC and IIT Bombay, respectively, for fellowships.

Keywords: blinking · colloidal quantum dots · $CsPbBr_3$ · luminescence · nanocrystals · perovskites

How to cite: *Angew. Chem. Int. Ed.* **2015**, *54*, 15424–15428
Angew. Chem. **2015**, *127*, 15644–15648

[1] C. K. Møller, *Nature* **1958**, *182*, 1436–1436.
[2] C. R. Kagan, D. B. Mitzi, C. D. Dimitrakopoulos, *Science* **1999**, *286*, 945–947.
[3] a) A. Kojima, K. Teshima, Y. Shirai, T. Miyasaka, *J. Am. Chem. Soc.* **2009**, *131*, 6050–6051; b) L. Etgar, P. Gao, Z. Xue, Q. Peng, A. K. Chandiran, B. Liu, M. K. Nazeeruddin, M. Grätzel, *J. Am. Chem. Soc.* **2012**, *134*, 17396–17399; c) M. M. Lee, J. Teuscher, T. Miyasaka, T. N. Murakami, H. J. Snaith, *Science* **2012**, *338*, 643–647; d) J. A. Christians, R. C. M. Fung, P. V. Kamat, *J. Am. Chem. Soc.* **2014**, *136*, 758–764; e) S. D. Stranks, H. J. Snaith, *Nat. Nanotechnol.* **2015**, *10*, 391–402.
[4] a) L. C. Schmidt, A. Pertegás, S. González-Carrero, O. Malinkiewicz, S. Agouram, G. Mínguez Espallargas, H. J. Bolink, R. E. Galian, J. Pérez-Prieto, *J. Am. Chem. Soc.* **2014**, *136*, 850–853; b) L. Protesescu, S. Yakunin, M. I. Bodnarchuk, F. Krieg, R. Caputo, C. H. Hendon, R. X. Yang, A. Walsh, M. V. Kovalenko, *Nano Lett.* **2015**, *15*, 3692–3696; c) F. Zhang, H. Zhong, C. Chen, X.-g. Wu, X. Hu, H. Huang, J. Han, B. Zou, Y. Dong, *ACS Nano* **2015**, *9*, 4533–4542; d) H. Huang, A. S. Susha, S. V. Kershaw, T. F. Hung, A. L. Rogach, *Adv. Sci.* **2015**, DOI: 10.1002/advs.201500194.
[5] a) M. A. Hines, P. Guyot-Sionnest, *J. Phys. Chem.* **1996**, *100*, 468–471; b) X. Peng, M. C. Schlamp, A. V. Kadavanich, A. P. Alivisatos, *J. Am. Chem. Soc.* **1997**, *119*, 7019–7029; c) B. O. Dabbousi, J. Rodriguez-Viejo, F. V. Mikulec, J. R. Heine, H. Mattoussi, R. Ober, K. F. Jensen, M. G. Bawendi, *J. Phys. Chem. B* **1997**, *101*, 9463–9475; d) A. L. Rogach, N. Gaponik, J. M. Lupton, C. Bertoni, D. E. Gallardo, S. Dunn, N. Li Pira, M. Paderi, P. Repetto, S. G. Romanov, C. O'Dwyer, C. M. Sotomayor Torres, A. Eychmüller, *Angew. Chem. Int. Ed.* **2008**, *47*, 6538–6549; *Angew. Chem.* **2008**, *120*, 6638–6650; e) K. Bourzac, *Nature* **2013**, *493*, 283; f) D. V. Talapin, J. Steckel, *MRS Bull.* **2013**, *38*, 685–691; g) A. H. Khan, A. Dalui, S. Mukherjee, C. U. Segre, D. D. Sarma, S. Acharya, *Angew. Chem. Int. Ed.* **2015**, *54*, 2643–2648; *Angew. Chem.* **2015**, *127*, 2681–2686.
[6] L. Qu, X. Peng, *J. Am. Chem. Soc.* **2002**, *124*, 2049–2055.
[7] C. R. Kagan, C. B. Murray, M. Nirmal, M. G. Bawendi, *Phys. Rev. Lett.* **1996**, *76*, 1517–1520.
[8] a) M. Nirmal, B. O. Dabbousi, M. G. Bawendi, J. J. Macklin, J. K. Trautman, T. D. Harris, L. E. Brus, *Nature* **1996**, *383*, 802–804; b) H. Weller, *Angew. Chem. Int. Ed.* **1998**, *37*, 1658–1659; *Angew. Chem.* **1998**, *110*, 1748–1750; c) H. He, H. Qian, C. Dong, K. Wang, J. Ren, *Angew. Chem. Int. Ed.* **2006**, *45*, 7588–7591; *Angew. Chem.* **2006**, *118*, 7750–7753; d) Y. Chen, J. Vela, H. Htoon, J. L. Casson, D. J. Werder, D. A. Bussian, V. I. Klimov, J. A. Hollingsworth, *J. Am. Chem. Soc.* **2008**, *130*, 5026–5027; e) P. Tyagi, P. Kambhampati, *J. Phys. Chem. C* **2012**, *116*, 8154–8160; f) A. Hazarika, A. Layek, S. De, A. Nag, S. Debnath, P. Mahadevan, A. Chowdhury, D. D. Sarma, *Phys. Rev. Lett.* **2013**, *110*, 267401; g) A. L. Routzahn, P. K. Jain, *Nano Lett.* **2015**, *15*, 2504–2509.
[9] a) M. Rodová, J. Brožek, K. Knížek, K. Nitsch, *J. Therm. Anal. Calorim.* **2003**, *71*, 667–673; b) C. C. Stoumpos, C. D. Malliakas, J. A. Peters, Z. Liu, M. Sebastian, J. Im, T. C. Chasapis, A. C. Wibowo, D. Y. Chung, A. J. Freeman, B. W. Wessels, M. G. Kanatzidis, *Cryst. Growth Des.* **2013**, *13*, 2722–2727.
[10] A. Nag, A. Kumar, P. P. Kiran, S. Chakraborty, G. R. Kumar, D. D. Sarma, *J. Phys. Chem. C* **2008**, *112*, 8229–8233.
[11] Its low sensitivity to moisture might arise from the coating hydrophobic capping layer on the NC surface, but needs to be studied further.
[12] a) C. Yu, Z. Chen, J. J. Wang, W. Pfenninger, N. Vockic, J. T. Kenney, K. Shum, *J. Appl. Phys.* **2011**, *110*, 063526; b) L. Y. Huang, W. R. L. Lambrecht, *Phys. Rev. B* **2013**, *88*, 165203; c) R. A. Jishi, O. B. Ta, A. A. Sharif, *J. Phys. Chem. C* **2014**, *118*, 28344–28349.
[13] a) F. Deschler, M. Price, S. Pathak, L. E. Klintberg, D.-D. Jarausch, R. Higler, S. Hüttner, T. Leijtens, S. D. Stranks, H. J. Snaith, M. Atatüre, R. T. Phillips, R. H. Friend, *J. Phys. Chem. Lett.* **2014**, *5*, 1421–1426; b) J. S. Manser, P. V. Kamat, *Nat. Photonics* **2014**, *8*, 737–743.
[14] a) Y. Tian, A. Merdasa, M. Peter, M. Abdellah, K. Zheng, C. S. Ponseca, T. Pullerits, A. Yartsev, V. Sundström, I. G. Scheblykin, *Nano Lett.* **2015**, *15*, 1603–1608; b) X. Wen, A. Ho-Baillie, S. Huang, R. Sheng, S. Chen, H.-c. Ko, M. A. Green, *Nano Lett.* **2015**, *15*, 4644–4649.

Received: September 4, 2015
Published online: November 5, 2015

